

Analytical and Numerical Investigation of 3D Multilayer Detachment Folding

Naiara Fernández and Boris Kaus

1 Introduction

Folding is a common mode of deformation in geology when mechanically layered rocks are subjected to compression. They occur on a wide range of scales from mm-scale to 10's of kilometers in places where upper crustal rocks are compressed as a result of tectonic plate convergence (such as in the Zagros mountains, Iran). The physical instability that results in the formation of folds has been studied for different rheologies: e.g. elastic, viscous and visco-elastic [1], power law [2] and more recently, also for visco-elasto-plastic [3]. However, most of the studies focus on the problem of a competent layer embedded in a matrix [1] or the case of a multilayer system embedded in a matrix [4], and therefore they consider only two different material properties. This is appropriate for small-scale folds, but on a crustal scale it was recently demonstrated that the viscosity contrast between various sedimentary layers also plays an important role [3]. Here, we therefore focus on the case of a multilayer system overlying a matrix or lower detachment layer [4, 5] affected by gravity with three different material viscosities: lower detachment or salt layer (η_s), overlying weak layers (η_w) and competent layers (η_c).

N. Fernández (✉) · B. Kaus (✉)
Institute of Geosciences, Johannes Gutenberg University Mainz, J.-J.-Becher Weg 21,
55128 Mainz, Germany
e-mail: fernande@uni-mainz.de

B. Kaus
e-mail: kaus@uni-mainz.de

2 Methods

The equations that describe slow moving geological processes are the incompressible Stokes equations for layers with strongly varying (Newtonian) viscosity. These equations can be solved analytically for a multilayer set up (assuming small deformations), and numerically using a (parallel) finite element method.

The analytical solution we use is a thick plate stability analysis [6]. While thin plate is a valid approximation for one layer problem in which the shear stresses between the competent layer and matrix can be omitted in certain cases, the thick plate is a more suitable approach for the multilayer case where the shear stresses occurring at different interfaces cannot be ignored.

The numerical models are performed using Lithosphere and Mantle Evolution Model (LaMEM), which is a 3D finite element code that solves the governing equations in a velocity-pressure formulation on massively parallel supercomputers using iterative multigrid preconditioners. In the simulations shown here, we use higher-order elements in a Lagrangian manner and do not remesh which assures high accuracy.

3 Multilayer Folding Phase Diagrams

The 2D semi-analytical solution is used to create mechanical phase diagrams in the parameter space defined by two viscosity ratios ($R_1 = \eta_c / \eta_s$ and $R_2 = \eta_c / \eta_w$) that are larger than one in nature (Fig. 1). Such diagrams show that different multilayer

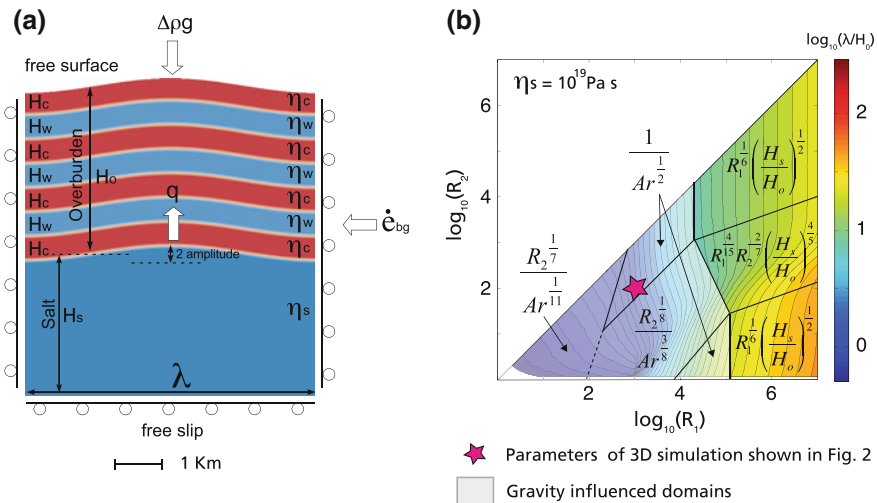


Fig. 1 **a** Model setup. **b** Phase diagram of normalized wavelength in the $R_1 - R_2$ space for $\eta_s = 10^{19} \text{ Pas}$, based on over 6000 results of the analytical solution. Parameters are defined in text

folding modes occur, each characterized with a scaling law for dominant wavelength (λ) and growth rate (q) that accounts for all model parameters (salt viscosity η_s , competent layer viscosity η_c , weak layer viscosity η_w , background strain rate $\dot{\epsilon}_{bg}$, density difference between rocks and air $\Delta\rho$, gravitational acceleration g , salt layer thickness H_s , and overburden thickness H_o). Four non-dimensional parameters occur: $R_1 = \eta_c / \eta_s$, $R_2 = \eta_c / \eta_w$, H_s / H_o and the Argand number [5] $Ar = (\Delta\rho g H_o) / (2 \eta_c \dot{\epsilon}_{bg})$.

Seven folding domains have been defined (Fig. 1). The three domains with the highest R_1 values are independent of the Argand number, and thus independent on gravity, but require unrealistically large viscosity contrasts (which are most likely limited to $10^4 - 10^5$). The other four folding domains within the low R_1 range all depend on the Argand number, and only two of them depend on R_2 . In the Argand number dependent domains the lower detachment layer must be below a critical value for the real detachment-folding mode to occur (defined as the folding mode controlled mainly by the H_s / H_o ratio). These results are in agreement with the folding modes defined for a two-layer system in [5]. For Earth-like viscosity contrasts if $R_1 < 10^5$, gravity is thus likely to play a role and as a consequence of the dependence in the Argand number, the deformation rate with which the mountain belt was deformed has an effect on the dominant wavelength that formed.

4 3D Numerical Simulations

We tested the validity of the phase diagrams beyond the initial folding stages by performing several 2D and 3D numerical forward simulations using LaMEM. The topography from the numerical simulations was extracted and analyzed during strain evolution, using both curvature analysis and 1D Fourier analysis both parallel and orthogonal to the compression orientation. The dominant wavelength predicted with the analytical methods was compared to the one obtained in the simulations, which shows that the calculated dominant wavelength is well preserved and clearly observable after a shortening of 30% (Fig. 2). Somewhat more pronounced than in 2D simulations, there is a range of wavelengths around the dominant wavelength that occurs. Moreover, the folds that develop have a range of aspect ratios that vary from elongated and sinusously perturbed to nearly egg-shaped. In addition, several high-resolution 3D numerical simulations were performed to study the evolution of 3D multilayer detachment folds under conditions that might be relevant to natural examples of fold-belts and study the interaction between different individual folds.

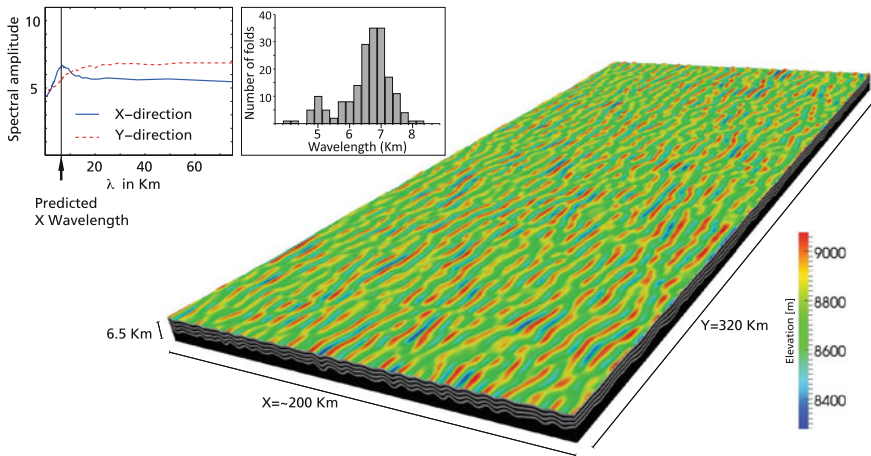


Fig. 2 Example of a 3D detachment folding simulation performed with LaMEM on 1024 cores. Resolution is $513 \times 513 \times 27$ nodes (high order Q2P-1 element). Inset shows the spectral analysis, as well as a histogram of fold spacing of the obtained topography

5 Conclusions

Several folding modes, that are applicable in a multilayer system overlying a lower detachment layer, have been defined. The equations of the dominant wavelength and growth rate for each of those domains and their boundaries were extracted using a 2D analytical solution. Analytically derived results were tested beyond the initial stages of folding by using numerical methods.

Numerical simulations show that the fold wavelength selected during strain in 3D multilayer folding is in agreement with the analytically calculated values. Furthermore, statistics of the numerical simulations exhibit a normally distributed fold wavelength around a dominant one in the direction parallel to the main compression and a large range of fold aspect ratios due to lack of wavelength selectivity in the direction orthogonal to the main compression. The different ways of interaction between folds as they laterally propagate, further influences the wide variety and range of final fold geometries.

Acknowledgments Funding was provided by the ERC under the European Community's Seventh Framework program (FP7/2007-2013) Grant agreement #258830. Numerical simulations were performed in JUQUEEN supercomputer of the Forschungszentrum Jülich, Germany

References

1. Biot, M. A. (1961). Theory of folding of stratified viscoelastic media and its implications in tectonics and orogenesis. *GSA Bulletin*, 72(11), 1595–1620.

2. Fletcher, R. C. (1974). Wavelength selection in the folding of a single layer with power-law rheology. *American Journal of Science*, 274(9), 1029–1043.
3. Yamato, P., et al. (2011). Dynamic constraints on the crustal-scale rheology of the Zagros fold belt. *Iranian Journal of Geology*, 39(9), 815–818.
4. Ramberg, H. (1964). Selective buckling of composite layers with contrasted rheological properties, a theory for simultaneous formation of several orders of folds. *Tectonophysics*, 1(4), 307–341.
5. Schmalholz, S. M., Podladchikov, Y. Y., & Burg, J. P. (2002). Control of folding by gravity and matrix thickness: Implications for large-scale folding. *Journal of Geophysical Research*, 107(B1), 2005.
6. Johnson, A. M., & Fletcher, R. C. (1994). *Folding of viscous layers*. New York: Columbia University Press.